

Immersed nano-sized Al dispersoids in an Al matrix; effects on the structural and mechanical properties by Molecular Dynamics simulations

H Chamati[‡], M S Stoycheva[§] and G A Evangelakis

Department of Physics, Solid State Division, University of Ioannina, P.O. Box 1186, GR-45110 Ioannina, Greece

E-mail: chamati@issp.bas.bg; gevagel@cc.uoi.gr

Abstract. We used molecular dynamics simulations based on a potential model in analogy to the Tight Binding scheme in the Second Moment Approximation to simulate the effects of aluminum icosahedral grains (dispersoids) on the structure and the mechanical properties of an aluminum matrix. First we validated our model by calculating several thermodynamic properties referring to the bulk Al case and we found good agreement with available experimental and theoretical data. Afterwards, we simulated Al systems containing Al clusters of various sizes. We found that the structure of the Al matrix is affected by the presence of the dispersoids resulting in well ordered domains of different symmetries that were identified using suitable Voronoi analysis. In addition, we found that the increase of the grain size has negative effect on the mechanical properties of the nanocomposite as manifested by the lowering of the calculated bulk moduli. The obtained results are in line with available experimental data.

PACS numbers: 61.46.+w,62.25.+g,63.20.Dj,81.07.-b

Submitted to: *J. Phys.: Condens. Matter*

[‡] Permanent address: Institute of Solid State Physics, 72 Tzarigradsko Chaussée, 1784 Sofia, Bulgaria

[§] Permanent address: Geophysical Institute, Acad. G. Bonchev str, bl.3, 1113 Sofia, Bulgaria

1. Introduction

Nanostructuring is usually used to improve the mechanical properties of bulk (coarse-grained) metals and alloys. In this context structures in the nanometer range as precipitates, different phases or dislocations arrays are introduced into the materials. The reduction of grain size down to the nanometer regime has opened new and fascinating avenues for research in several aspects of materials science. Nanocrystalline materials are believed to exhibit quite different responses under irradiation environments compared to coarser-grained materials. From theoretical point of view it is interesting to model nanocrystalline metals since the small grain size results in a cutoff of the typical length scale of the phenomena and structures that may appear during the deformation process. For a further discussion of mechanical properties of nanocrystalline metals see References [1, 2, 3] and references therein.

The investigation of the physical as well as chemical properties of metallic clusters received considerable attention in the last few decades (for a review on the experimental studies see Reference [4]). The size of these clusters is typically ranging from 1-100 nanometers, whence the name ‘nanoclusters’ is used for these particles. Because of their properties that are very different from their bulk or nanocrystalline counterparts they are very promising in many technological applications. Usually they adopt structures that are completely different from their bulk parents. It has been found both experimentally and analytically that they may exist in many different structures: icosahedral, decahedral, Marks polyhedra, etc. The change in the behaviour of these nanosized particles is originating mainly from their large surface to volume ratio, while the major contributions to the physical and chemical properties originate from their surfaces.

The interest in materials that are an assemblage of nanometer-sized particles, the so called nanocomposite, arises from the realization that by controlling their size we can alter a variety of physical, mechanical and chemical properties of the bulk materials (see Reference [5] and references therein).

According to the physical theory of strength the dispersion of crystalline structures inside a polycrystalline matrix promotes essential rise of strengthening and improves low temperature plasticity of the materials. Moreover, microcrystalline materials can exhibit superplasticity at high temperatures. High mechanical properties could be expected when extrapolating this tendency to nanocrystalline structures; however, as the amount of experimental data increases, it becomes obvious that only a few studies confirm such an assumption.

Small nano-sized particles dispersed homogeneously throughout the bulk of an alloy enhance its strength by impeding dislocation motion [2]. The dispersion of such grains is achieved either by mechanical mixing with the matrix material or by precipitation from a supersaturated solution. The former provides independent control of the size, type, morphology and volume fraction of the grains, called disperseoids. The effectiveness of ‘disperseoids’ depends on their size, spacing and distribution. The characteristics of the

interface separating the dispersoid and the matrix play a crucial role on the structural and mechanical properties of the nanocomposites.

In the present work we investigate the effects of Al dispersoids on an Al matrix. A nano-sized grain was placed at the center of a liquid Al matrix. Using Molecular dynamics we investigated the structural as well as the mechanical alterations of the Al matrix compared to Al bulk properties.

The paper is organized as follows. In Section 2 we present some thermodynamic quantities of the bulk aluminum along with the corresponding experimental data. In Section 3 we describe the dispersoids and we investigate their effects in a bulk aluminum matrix, to end up with a discussion that is given in Section 4.

2. Physical properties of bulk aluminum

It is known that interatomic potentials play a key role in any computer simulation in materials science. Much progress has been done on the development of semi-empirical interatomic potentials including the so-called ‘many-body interactions’. These terms are meant to take into account the local electronic density. Among several many-body potentials, the most popular are the embedded atom model (EAM), the Finnis-Sinclair potentials (FS) and the tight-binding potential in the second moment approximation. Though based on different approaches these models are shown to be equivalent [6] at least from the mathematical point of view.

In the present work, we choose a tight-binding potential in the second moment approximation, according to which the total energy of the system can be expressed as:

$$E = \sum_i \left[\sum_{j \neq i} A e^{-p(r_{ij}/r_0 - 1)} - \xi \sqrt{\sum_{j \neq i} e^{-2q(r_{ij}/r_0 - 1)}} \right], \quad (1)$$

where the first sum over j is a Born-Mayer type pairwise potential adapted for the description of the repulsive contributions, while the second one represents the band-structure term. In the above expression (1), r_{ij} is the distance between atoms i and j , while the interactions up to fifth neighbors were taken into account. The adjustable parameters A , ξ , p , q and r_0 in this approach have been determined through fitting to the total energy of the system as computed by first-principles APW calculations and taking into account the experimental values of the cohesive energy, the lattice constant and the structural stability of the ground state (see details in Reference [7]). The values of the parameters are given in Reference [7]: $A = 0.05504$ eV, $\xi = 0.9564$ eV, $p = 10.9011$, $q = 1.5126$ and $r_0 = 2.8310$ Å. We note that this model is composed of exponential functions resulting in high numerical reproducibility.

As a test of the quality of our parameters, in a previous paper [7], we calculated some bulk properties: bulk moduli, elastic constants, phonon density of states at room temperature, temperature dependence of the lattice constant as well as the mean square-displacement. The obtained results were found to be in good agreement with the corresponding experimental values.

Table 1. Computed properties of bulk Al along with experimental, *ab initio* data, and EAM potential results [8]

	Experiment or <i>ab initio</i>	Present work	EAM (Reference [8])
<u>Lattice properties:</u>			
$a_0(\text{\AA})$	4.05 ^a	3.995	4.05
$E_0(\text{eV/atom})$	-3.36 ^b	-3.34	-3.36
$B(10^{12}\text{Pa})$	0.79 ^c	0.73	0.79
$c_{11}(10^{12}\text{Pa})$	1.14 ^c	0.92	1.14
$c_{12}(10^{12}\text{Pa})$	0.619 ^c	0.63	0.616
$c_{44}(10^{12}\text{Pa})$	0.316 ^c	0.48	0.316
<u>Phonon frequencies:</u>			
$\nu_L(X)(\text{THz})$	9.69 ^d	9.70	9.31
$\nu_T(X)(\text{THz})$	5.80 ^d	6.25	5.98
$\nu_L(L)(\text{THz})$	9.55 ^d	9.52	9.64
$\nu_T(L)(\text{THz})$	4.19 ^d	4.10	4.30
$\nu_L(K)(\text{THz})$	7.59 ^d	7.45	7.30
$\nu_{T_1}(K)(\text{THz})$	5.64 ^d	5.45	5.42
$\nu_{T_2}(K)(\text{THz})$	8.65 ^d	8.40	8.28
<u>Vacancy:</u>			
$E_v^f(\text{eV})$	0.65 ^e	1.28	0.68
<u>Surfaces:</u>			
$\gamma_s(110)(\text{mJ/m}^2)$	1200 ^f	1410	1006
$\gamma_s(100)(\text{mJ/m}^2)$	1200 ^f	1320	943
$\gamma_s(111)(\text{mJ/m}^2)$	1200 ^f	1290	870

^a Reference [9]^b Reference [10]^c Reference [11]^d Reference [12]^e Reference [13]^f Reference [14]

Using the above interatomic potential, we performed additional molecular dynamics simulations in the isothermal canonical ensemble (NVT) using the NOSE daemon to control the temperature and the Verlet algorithm with a time step of 5 fs for the integration of the equations of motion. The system was made up of 4000 particles arranged in the appropriate lattice structure.

Here we present further results (see Table 1) computed within the framework of this model. A comparison of our results with experimentally available values shows that our model reproduces quite well the equilibrium properties, elastic constant (except C_{44}) as well as the surface energies. The elastic constants are given here for sake of completeness.

In Figure 1, we present the phonon-dispersion curves for aluminum at room temperature, along with the corresponding neutron scattering data [15]. We observe

a remarkable accuracy of our model for the high-symmetry branches and the cutoff frequency except for a slight overestimation of about 1 THz for the transverse mode along [100] and T_1 , and L along [110] direction, in the vicinity of the point X. This is compatible with the inaccuracy found in our calculated value of C_{44} .

In addition, we calculated the surface energies for the three low indexed surfaces. The values we obtained are slightly higher than the experimental data [13], a result that is opposite from what it is usually found using EAM type potentials (see Reference [8] for more details), but in reasonable agreement with the experimental and theoretical data. On the contrary, the evaluation of the vacancy formation energy yielded a value that is not close to the experimental data. This result has to be attributed to the charge transfer between neighbors around the vacancy, an effect that requires different approach in order to be treated properly; in our model the electronic contributions are incorporated into the second term of the potential energy functional and therefore cannot be used to take into account eventual electronic modifications.

Moreover we estimated the melting temperature of our potential model for aluminum using the Lindemann's criterion [16]. According to this criterion, at the melting temperature the average amplitude of vibration is about 8% of the nearest-neighbor distance. A linear extrapolation of our atomic mean-square displacement results [7] gives a melting temperature of 960 K, consistent with the experimental value of 933 K of high-symmetry crystal structures.

Turning our attention to the mechanical properties, we calculated the elastic constants since they yield valuable information concerning the strength and the stability of materials. A knowledge of their behaviour over a wide range of temperature is of a fundamental importance in characterising a large number of mechanical, electric, optical and thermodynamic properties. The molecular dynamics computation of isothermal elastic constants, c_{ijkl}^T , is given by the following expressions [17, 18]

$$\begin{aligned} c_{11}^T &= \frac{1}{Vk_B T} \left(\langle \varphi_{ii} \rangle^2 - \langle \varphi_{ii}^2 \rangle \right) + \frac{1}{V} \langle \varphi \rangle + \frac{2Nk_B T}{V} \\ c_{12}^T &= \frac{1}{Vk_B T} \left(\langle \varphi_{ii} \varphi_{jj} \rangle - \langle \varphi_{ii} \rangle \langle \varphi_{jj} \rangle \right) + \frac{1}{V} \langle \varphi_{ijj} \rangle \\ c_{44}^T &= \frac{1}{Vk_B T} \left(\langle \varphi_{ij} \rangle^2 - \langle \varphi_{ij}^2 \rangle \right) + \frac{1}{V} \langle \varphi_{ijij} \rangle + \frac{Nk_B T}{V}, \end{aligned}$$

where V is the volume of the simulation box and k_B the Boltzmann constant; T is the temperature; φ_{ij} and φ_{ijkl} are the first and the second derivatives of the potential energy φ with respect to the strain tensor components η_{ijkl} respectively and the brackets denote canonical averages. Thermodynamic averages were obtained from equilibrium molecular dynamics trajectories that lasted 50 000 time steps.

Here we present only results referring to the temperature dependence of the bulk modulus (Figure 2). Note that the values of this thermoelastic quantity were obtained using the relationship $B = (c_{11} + 2c_{12})/3$ valid for cubic lattices [19]. We found a fairly good agreement with experimental values [20] and theoretical calculations [21].

It comes out that the present model reproduces quite satisfactorily the main features

of the bulk Al and it can therefore be used for simulations of at least the characteristic properties of aluminum nanostructures.

3. Effects of nano-Al dispersoids on the bulk system

3.1. Molecular dynamics procedure

A criterion that is helpful in finding the most stable configuration of a dispersoid (nanocluster) is the use of the Wulff construction that was developed for finding the equilibrium shape of a quasi-crystal made of a given number of atoms by minimizing its surface energies. In the present study the number of atoms has been chosen to correspond to the magic numbers identifying icosahedra [22]. These are structured in shells. An icosahedra with k shells has

$$N(k) = \frac{10}{3}k^3 - 5k^2 + \frac{11}{3}k - 1 \quad (2)$$

atoms (so the series of magic numbers is 1, 13, 55, 147, ...) exhibiting 20 triangular facets of side k (for more details see [22]).

Using different approaches, various aluminum cluster sizes (Al_n , where n indicates the number of atoms composing the cluster) are investigated in the literature. It has been found using an *ab initio* study [23] that the Al_{55} cluster presents substantial structural distortions in its lowest-energy configuration with respect to the highly symmetric icosahedral. Several inequivalent and energetically degenerated structures were found. The origin of this degeneracy is traced to the short range effective interatomic potential. Using molecular dynamics investigation combined with a simulated annealing technique, Reference [24] gave results referring to the structural and dynamical properties of Al_n clusters ($n = 13, 55$, and 147) that were found to agree with *ab-initio* calculations. Very recently the electronic and thermodynamic properties of Al_n clusters ($n = 55, 147$, and 309) were determined. It was found that these clusters have melting points and bulk moduli lower than those corresponding to the bulk Al, while they exhibit enhanced low and high energy phonon densities of states [25]. The calculated electronic density of states revealed significant enhancement at energies around the Fermi level, indicating clear quantum confinement. This is due to the charge transfer from the inner atoms towards the surface atoms [25].

To obtain the lowest-energy configuration of each cluster we used a simulated annealing and quenching technique. These techniques are the best available procedures to find the global and local minima in complicated situations. They allow us to test the results by varying cooling rates and starting configurations. We start with fcc clusters consisting of a number of atoms corresponding to a magic number (given by Equation (2)) of the icosahedral structure. We heat the initially constructed clusters up to temperatures that are higher than the melting point. The resulting liquid is subsequently quenched in order to minimize the energy. The procedure is repeated several times and the coordinates of the quenched cluster were saved. Finally, the

cluster with the lowest energy is kept for further study. Let us emphasize that these clusters are found to have an icosahedral-like structure as expected.

In order to investigate the effects of the nano-al dispersoids in the Al matrix, we choose the preparation of a liquid phase by starting with an fcc lattice corresponding to the aluminum matrix. The lattice constant has been adjusted to have zero pressure for the liquid at 2000K, temperature at which the system was thermalized for 20 000 time steps. Subsequently, we placed five different nano-sized icosahedral (Al_n) grains (dispersoids), consisting of $n = 55, 147, 309, 561$ and 923 atoms, at the center of the resulting liquid, forming five different initial configurations of nano-composites. Care has been taken when placing the grains inside the matrix in order to keep the same orientation for all grains and be able to compare the effects of grain size on the matrix eliminating the effect that could possibly be induced by their different orientations. Next, the samples were cooled down to 500K and allowed to equilibrate for 500 000 time steps. During this time the dispersoids were fixed at their initial positions. For these final configurations, we investigated the structural and mechanical properties.

To facilitate the analysis of the local atomic order of our final configurations we used the algorithm proposed in Reference [26]. According to this algorithm the bonds between an atom and its ‘relevant’ neighbors are examined to determine the crystal structure using a Voronoi construction with self-adjusting cutoff to recognize the nearest neighbors. This method classifies the atoms into four classes: bcc, fcc, hcp and icosahedral. Additional details and advantages of the method can be found in Reference [26].

3.2. Results

In Figure 3 we present the average pair distribution functions (obtained from the molecular dynamic runs) of the various Al samples with grains inside. The index n in Al_n indicates the number of atoms forming the dispersoids. The configuration labeled as Al_{000} corresponds to the free of grains case and it serves as a reference configuration. The peaks could be related one by one to the different coordination shells of the polycrystalline matrix. We observe that the grain size affects the structure of the equilibrated aluminum matrix at 500K. More specifically, the reference matrix (Al_{000}) has more pronounced peaks than the others and its pair distribution function is more similar to the fcc structure. This is confirmed by the Voronoi analysis shown in Figure 4. By increasing the grain size we diminish the ratio between the grain size and the aluminum matrix. The size of the grain affects its structural as well as mechanical properties. It comes out that although the mean coordination number remains more or less the same, the number of the atoms having more neighbors changes. As a result different local structures appear: fcc, bcc, hcp and icosahedral in different proportions. This is due to the embedded icosahedral grains. The largest grain i.e. the one with 923 atoms affects the system more drastically leading to an (amorphous) glassy structure, while the coordination number in this case is lower than in the cases with smaller grains.

The effects of the grain size on the mechanical properties of the polycrystalline reference configuration have been verified by calculating the bulk modulus of the final configurations. We consider that this quantity can be used to obtain an evidence of the effect of the grain size on the mechanical properties of the system, at least qualitatively. The bulk modulus is evaluated using

$$B = V \frac{\partial^2 E}{\partial V^2},$$

expressing the variation of the potential energy E with respect to the volume V of a given ‘static’ configuration at the minimum. The calculations were carried out on the final configurations obtained from the quenched equilibrated systems at 500K. The results are depicted in Figure 5. We see that the bulk modulus decreases as the grain size increases, indicating softening of the matrix, in agreement with experimental observations [27].

The final configurations we used are shown in Figure 8. We observe that the atoms surrounding the grains order following their icosahedral structure, while the atoms far from the grains form different local structures in agreement with the Voronoi analysis described above. We note also that the atoms around the grains form icosahedral shells, increasing in this way the original size of the dispersoid.

In order to test whether our results depend on the size of the cell and the simulation time we performed molecular dynamics using a large system of 10976 atoms and an icosahedral nanoparticle of 923 atoms immersed at its center. The corresponding pair distribution function, Figure 6, exhibits the characteristic peaks of an fcc structure, while the Voronoi analysis, given in Figure 7, reveals that the system orders in locally different structures. The situation is similar to the system of 4000 atoms with Al_{309} . By computing the bulk modulus we find $B = 61.58$ GPa for the unrelaxed and $B = 64.61$ GPa for the relaxed lattices.

4. Discussion

We presented an extensive Molecular Dynamics study of the physical properties of bulk aluminium and the effect that is induced by nanosized Al dispersoids immersed in an Al matrix. The simulations were based on an interatomic potential in analogy to Tight-Binding Scheme in the second moment approximation. We computed several properties, like bulk modulus and its temperature dependence, elastic constants, phonon frequencies, vacancy formation energy and surface energies. The obtained results show good agreement between simulation and available experimental data for the bulk case.

Considering that our potential is able to describe well not only the bulk properties of the fcc aluminum but also other structures, at least qualitatively, we simulated aluminum matrices containing Al icosahedral grains of different sizes. From the computed pair distribution functions we found several peaks that are not characteristic of any simple structure yielding a system that exhibits a certain order that is not trivial to be identified. The application of a Voronoi analysis yielded a clearer picture of the structure of the aluminum nanocomposites. We found that the system has a polycrystalline

structure with different regions of local order that were identified to be: fcc, bcc, hcp and icosahedral. The atoms in the vicinity of the icosahedral grains organize themselves in shells following the icosahedral structure. This result was confirmed by visualising the final equilibrium configurations of the molecular dynamics simulations at finite temperature. We note here that upon releasing the nanoparticles the system reorders quickly in an fcc like structure.

In addition, we found that the increase of the grain size has negative effect on the mechanical properties of the nanocomposites as manifested by the lowering of the calculated corresponding bulk moduli.

Finally we would like to mention that it would be interesting to extend the present study to other materials, in particular magnetic systems and to investigate their effects on the aluminum matrix, *e.g* Nickel dispersoids.

Acknowledgments

This work was supported by the European grant HPRN-CT-2000-00038.

References

- [1] Morris D G and Morris M A 1997 *Mater. Sci. Forum* **235–238** 861.
- [2] Hauert R and Patscheider J 2000 *Adv. Eng. Mater.* **2** 247.
- [3] Cheng D, Trapaga G, McKelliget J W and Lavernia E J 2003 *Modelling Simul. Mater. Sci. Eng.* **11** R1.
- [4] Marks L D 1994 *Rep. Prog. Phys.* **57** 603.
- [5] Murthy B S, Datta M K and Pabi S K 2003 *Sādhanā* **28** 23.
- [6] Voter A F 1994 *The embedded-atom model*, in: *Intermetallic Compounds: Vol. 1, Principles*. ed. by J H Westbrook and R L Fleisher (Wiley, New York).
- [7] Papanicolaou N I, Chamati H., Evangelakis G A and Papaconstantopoulos D A 2003 *Comput. Mater. Sci.* **27** 191.
- [8] Mishin M, Farkas M, Mehl M J and Papaconstantopoulos D A 1999 *Phys. Rev. B* **59** 3393.
- [9] Kittel C 1986 *Introduction to Solid State Physics* (Wiley-Interscience, New York).
- [10] Weast R C (ed.) 1986 *Handbook of Chemistry and Physics* (CRC, Boca Raton).
- [11] Smith C J (ed.) 1976 *Metal Reference Book*, 5th ed. (Butterworth, London).
- [12] Simons G and Wang H 1977 *Single Crystal Elastic Constant and Calculated Aggregate Properties* (MIT Press, Cambridge).
- [13] Tyson W R and Miller W A 1977 *Surf. Sci.* **62** 267.
- [14] Schaefer H E, Gugelmeier R, Schmolz M and Seeger A 1987 *Mater. Sci. Forum* **15-18** 111.
- [15] Stedman R and Nilsson G 1966 *Phys. Rev.* **145** 491.
- [16] Lindemann A 1910 *Z. Phys.* **11** 609.
- [17] Squire D R, Holt A C and Hoover W G (1969) *Physica* **42** 388.
- [18] Zhou Z and Joós B 2002 *Phys. Rev. B* **66** 054101.
- [19] Mehl M J, Klein B M and Papaconstantopoulos D A 1994 in: *Intermetallic Compounds: Vol. 1, Principles*. ed. by J H Westbrook and R L Fleisher (Wiley, New York).
- [20] Tallon J L and Wolfenden A 1979 *J. Phys. Chem. Solids* **40** 831.
- [21] Zoli M and Bortolani V 1990 *J. Phys.: Condens. Matter* **2** 525.
- [22] Martin T P 1996 *Phys. Rep.* **273** 199.
- [23] Yi J Y, Oh D J and Bernholc J 1991 *Phys. Rev. Lett.* **67** 1594.
- [24] Sun D Y and Gong X G 1997 *Phys. Rev. B* **57** 4730.

- [25] Mitev P, Papageorgiou D G, Lekka Ch E and Evangelakis G A 2003 *Surf. Sci. to appear 2004*.
- [26] Stankovic I., Kröger M. and Hess S. 2002 *Comp. Phys. Comm.* **145** 371.
- [27] Bonetti E, Pasquini L and Sampaolesi E 1997 *NanoStructured Materials* **9** 611.

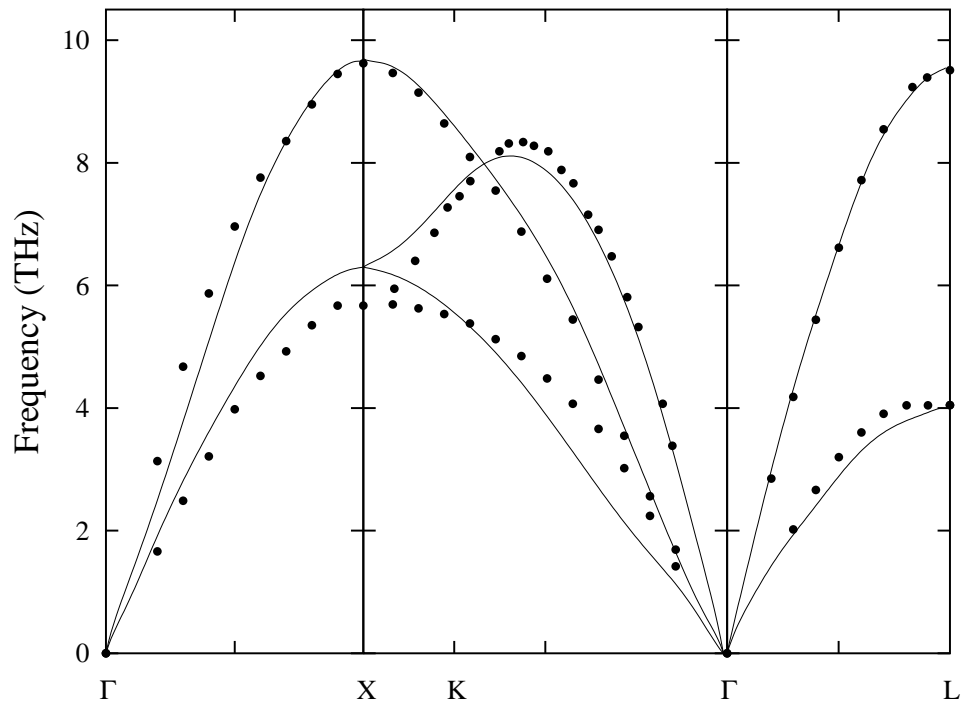


Figure 1. Phonon dispersion curves of Al at 300K. Solid lines correspond to molecular dynamics simulations, filled circles refer to experimental data from Reference [15].

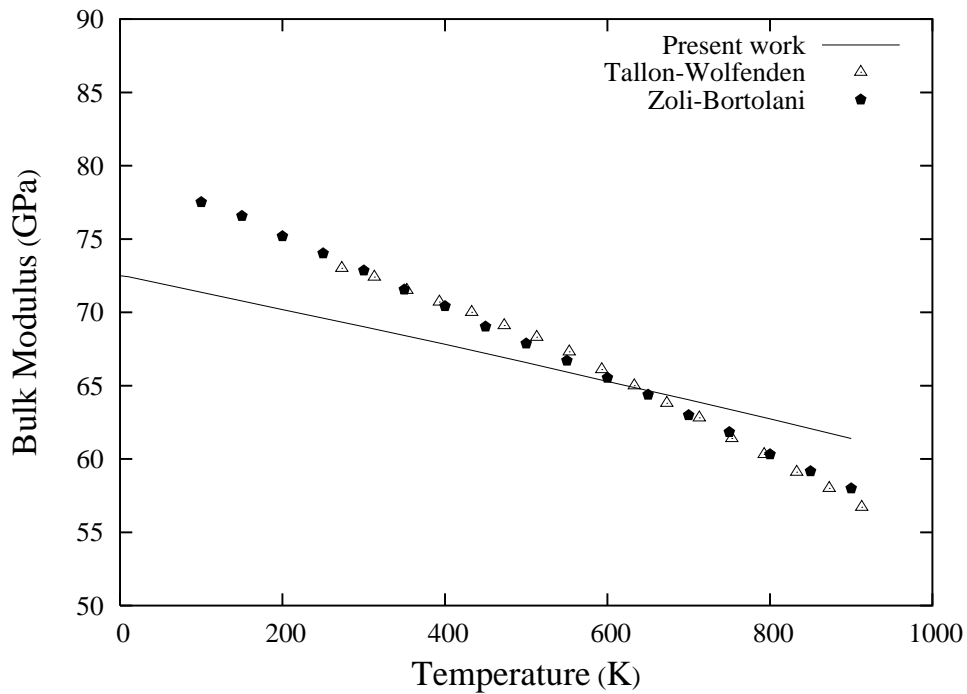


Figure 2. Temperature dependence of the isothermal bulk modulus of aluminum. The experimental results are taken from Reference [20] and the theoretical from Reference [21].

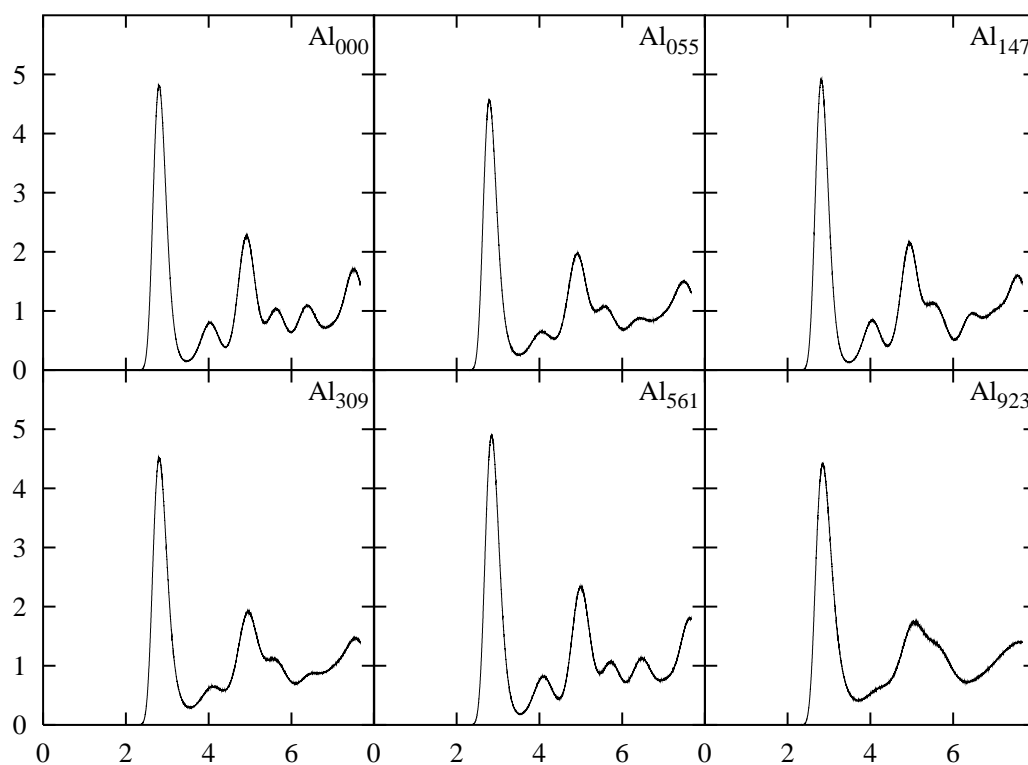


Figure 3. Radial distribution functions of the equilibrated aluminum systems containing various dispersoids

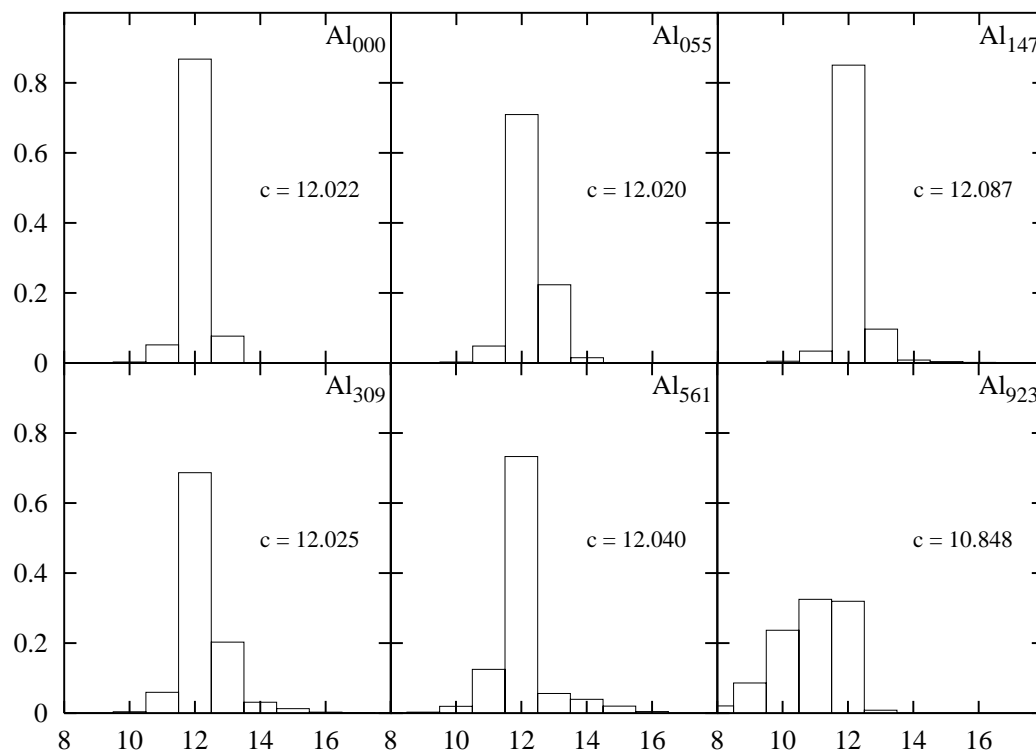


Figure 4. Coordination histograms obtained from Voronoi structural analysis of the final configurations. The quantity c is the mean coordination number.

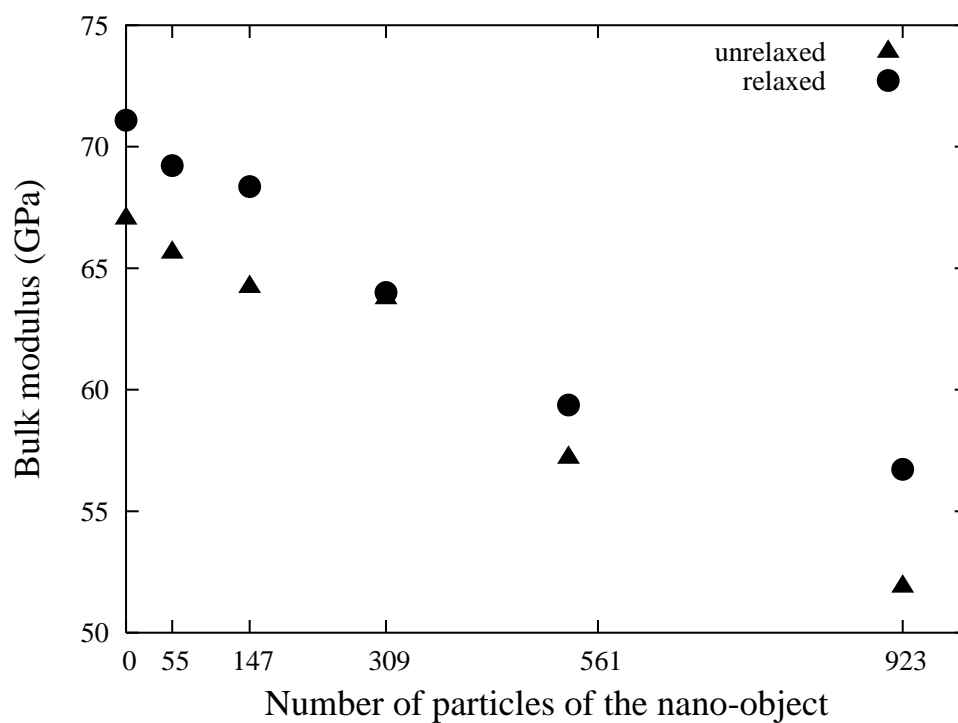


Figure 5. Static bulk moduli of the various final configurations.

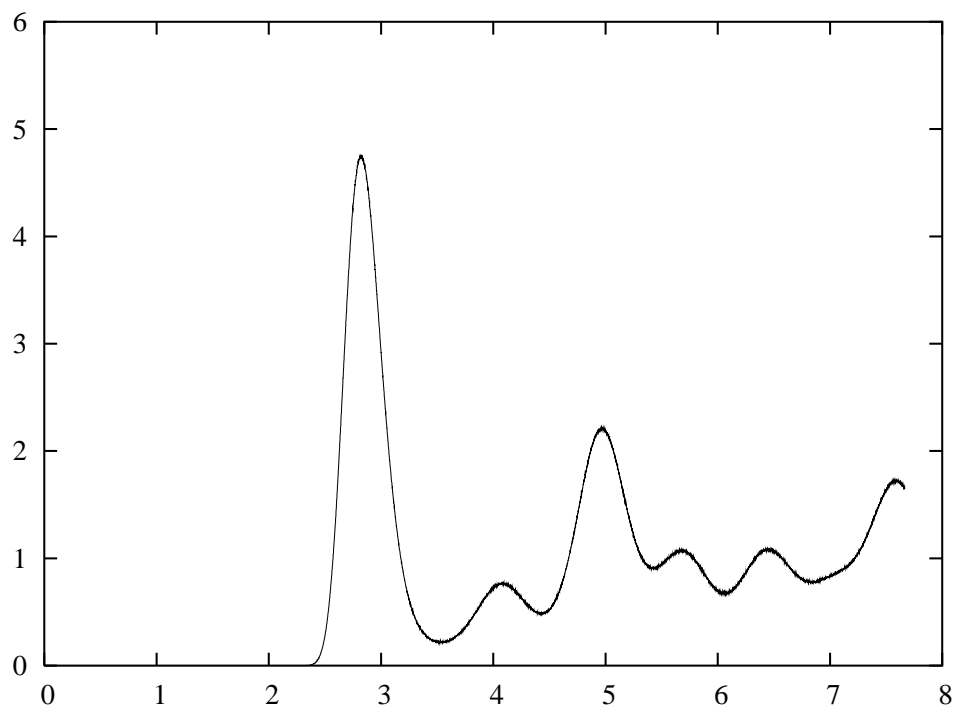


Figure 6. The same as in Figure 3 for the large system.

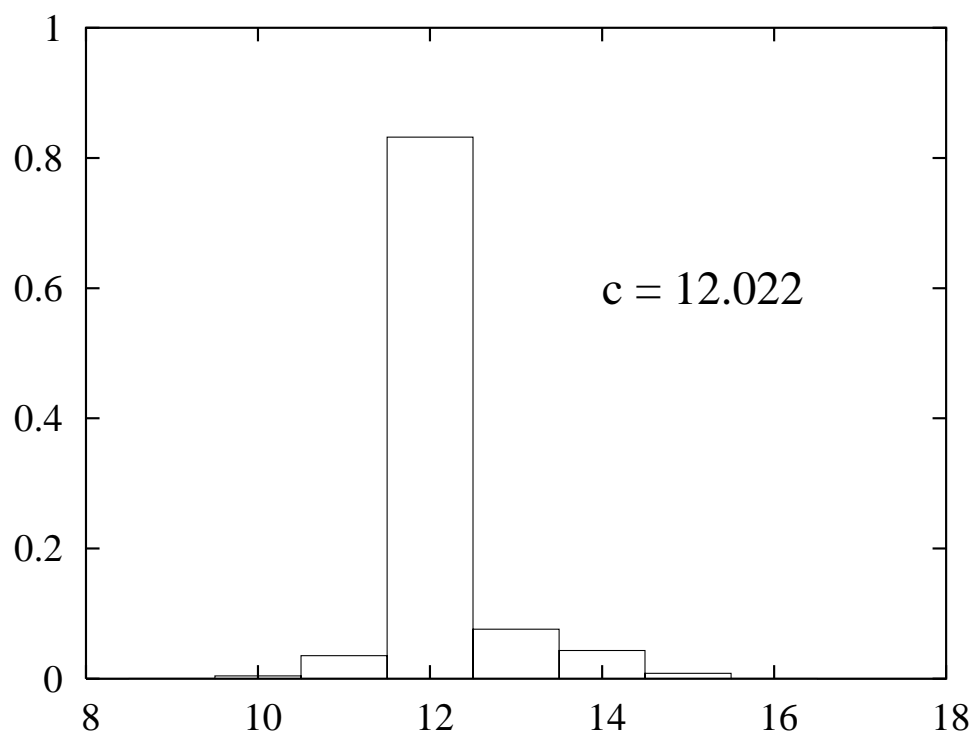


Figure 7. The same as Figure 4 for the large system.

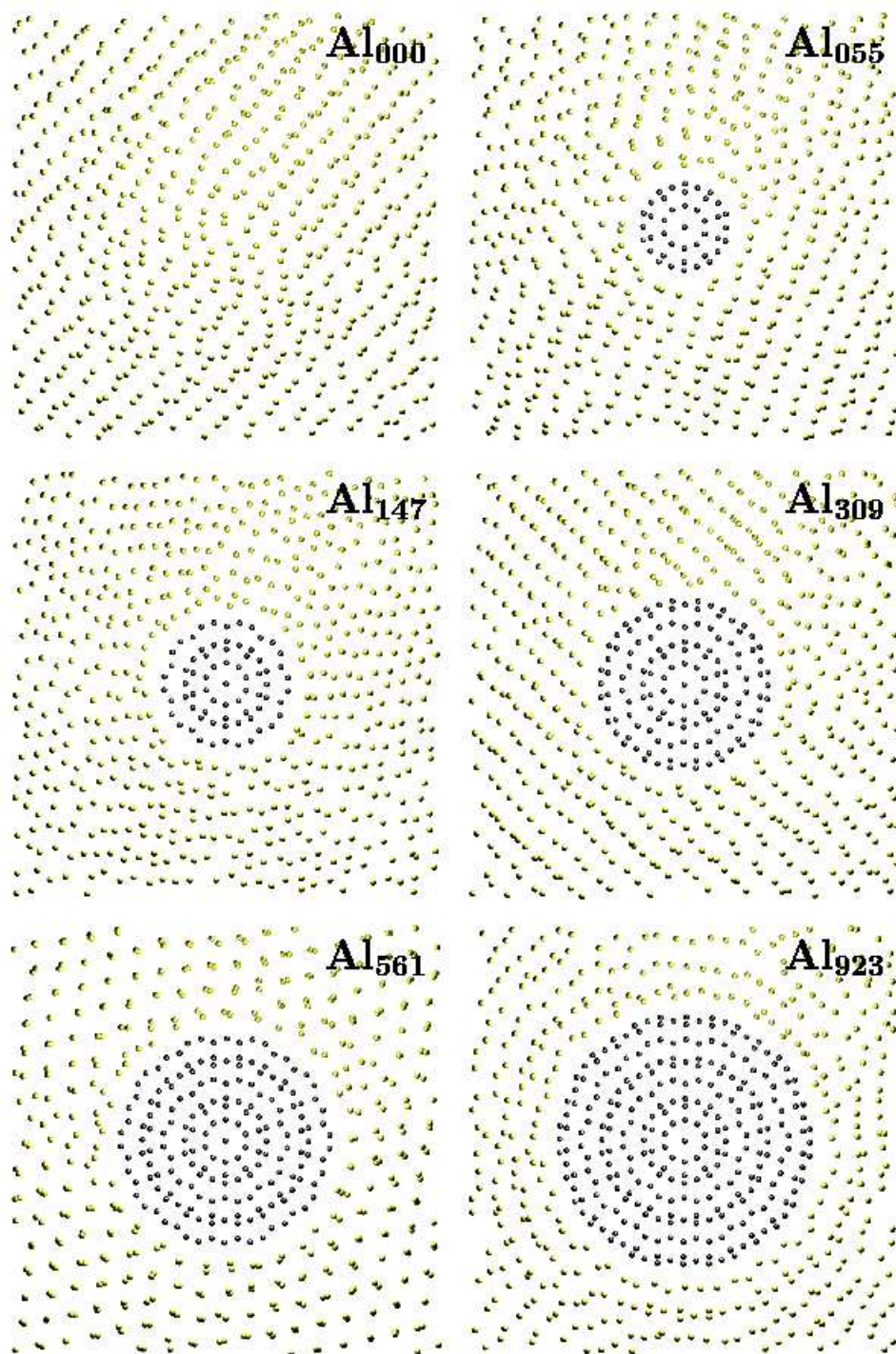


Figure 8. Selected snapshots of the final configurations showing the dispersoids inside the simulated systems.